 https://doi.org/10.3311/PPch.42778

Periodica Polytechnica Chemical Engineering, 70(1), pp. 54–63, 2026

Emerging Structures of Tin-based Nanocluster via DFT-Electronic Analysis: Saving Energy in SnC through Li-Replacement with B, Al or Ga in Batteries

Fatemeh Mollaamin[1*], Majid Monajjemi[2]

[1] Department of Biomedical Engineering, Faculty of Engineering and Architecture, Kastamonu University, 37150 Kastamonu, Turkey
[2] Department of Biology, Faculty of Science, Kastamonu University, 37100 Kastamonu, Turkey
[*] Corresponding author, e-mail: fmollaamin@kastamonu.edu.tr

Received: 09 November 2025, Accepted: 29 January 2026, Published online: 20 February 2026

Abstract

Tin carbide (SnC) has been developed and characterized as an anode electrode for lithium, boron , aluminum and gallium on batteries, forming Sn(Li)C, Sn(B)C, Sn(Al)C, and Sn(Ga)C nanoclusters. A comprehensive study on energy savings with Sn(Li)C, Sn(B)C, Sn(Al)C, and Sn(Ga)C complexes was conducted using computational approaches, including density state analysis of charge density differences , total density of states and electron localization function for hybrid clusters of Sn(Li)C, Sn(B)C, Sn(Al)C, and Sn(Ga)C. A small amount of Li, B, Al, or Ga entering the Si-C layer could enhance the structural stability of the electrode material at high multiplicity, thus improving the capacity retention rate. Higher Si/C content can increase battery capacity through Sn(Li)C, Sn(B)C, Sn(Al)C, and Sn(Ga)C nanoclusters for energy storage processes and enhance rate performances by improving electrical conductivity. The results showed that Li, B, Al, and Ga are chemisorbed on the SnC, with electronic charge transferring from the decorating atom to the SnC. Furthermore, the SnC anode material may improve cycling consistency by reducing electrode degradation and increasing capacity due to higher surface capacitive effects. This research aims to provide insight into the investigation of boron, aluminum, and gallium in energy-saving materials and contribute to the advancement of future research in this area.

Keywords

Li-group battery, heterocluster SnC-based anode, energy storage, boro-group substitution, electronic states

1 Introduction

Since the 1990s, when lithium-ion batteries (LIBs) began to be used commercially, researchers have shown a significant interest in anodes made from tin, antimony, and germanium. These materials are considered promising options for future LIBs because they have the ability to store a large amount of energy, operate at the appropriate voltage levels, and are relatively abundant in nature. Concurrently, concerns regarding the limited availability of lithium have sparked a resurgence in interest in sodium-ion batteries. Tin, antimony, and germanium can also create alloys with sodium, positioning them as strong candidates for high-performance sodium-ion batteries [1].

Recently, a basic understanding of boron and boron-based materials is first introduced. Subsequently, the recent research progress on the application of boron in each component of the lithium-battery (LB) is summarized, aiming to understand the hybrid forms of boron and their potential for use in LB materials. Finally, some new strategies and perspectives on the application of boron in LB materials are proposed. Here, the aim is to provide a clear insight on the study of boron in energy storage materials and contribute to the promotion of further research in this area [2].

The scientists have explored various aluminum battery technologies, with a primary focus on Al-ion and Al-sulfur batteries. They also examined alternative applications such as Al redox batteries and supercapacitors, with pseudocapacitance emerging as a promising method for accommodating Al^{3+} ions [3]. The abundance of aluminum, its superior charge storage capacity using Al^{3+} ions in comparison to Li^{+} ions, and a fourfold greater volumetric capacity for Al anodes avoid the safety concerns associated with alkali metals [3]. Ga-based liquid metals (LMs) possess self-healing capability, fluidity, and metallic advantages so they have been employed as self-healing skeletons or interfacial protective layers to

Cite this article as: Mollaamin, F., Monajjemi, M. "Emerging Structures of Tin-based Nanocluster via DFT-Electronic Analysis: Saving Energy in SnC through Li-Replacement with B, Al or Ga in Batteries", Periodica Polytechnica Chemical Engineering, 70(1), pp. 54–63, 2026. https://doi.org/10.3311/PPch.42778

minimize the negative impact of volume expansion or dendritic growth on the electrode materials [4–6].

Large volume variation during charge/discharge of silicon nanostructures applied as the anode electrodes for high energy LIBs has been considered the most critical problem, inhibiting their commercial applications. Searching for alternative high-performance anodes for LIBs has been emphasized [7].

Tin and tin compounds, a promising electrode material for high-capacity LIBs anodes, attracted much attention because of its large capacity and remarkably fast charge/discharge kinetics. Multivalent-ion batteries are of interest as potential alternatives to LIBs because they have a higher energy density and are less prone to safety hazards [8].

Although Sn is a promising anode material for LIBs, fundamental limitations such as large volume expansion during charge/discharge cycle and confined electronic conductivity restrict its practical efficiency. Therefore, the researhers performed a new material architecture and manufacturing approach of LIB anodes using Sn and hard carbon which is generated by physical vapor deposition. The improved anodes have been applied to produce cells with a Li-ion electrolyte using a specific fabrication status [9]. A number of electrode materials with high theoretical capacity, including Sn, Si, Li metal anode, and S cathode materials, have been explored [4]. Recently, a review article discussed the latest advances in the development of Sn-based anodes for Na-ion batteries to understand in detail the obstacles hindering the full utilization of these materials [10].

In addition, it has been theoretically proven that tin carbide monolayers (SnC-ML) decorated with alkali metals (Li, Na, and K) are also promising hydrogen-storage materials [11]. They reported hydrogen storage in tin carbide monolayers implanted with lithium, sodium, and potassium using a density-functional study. It was indicated that the most stable adsorption site for these alkali metal atoms on the tin carbide is above a tin atom. The results exhibited that the alkali metal atoms are chemisorbed on the tin carbide and that electronic charge is transferred from the decorating atom to the the tin carbide [11].

In comparison to other alloying anodes, such as non-metals silicon, phosphorus, germanium and even metals like tin, bismuth and antimony, gallium anode shows a lower capacity. Nevertheless, with a low melting point of 29.8 °C and soft mechanical property, gallium is in liquid form at ambient temperature. The flowing feature of liquid enables an arbitrary deformation of gallium to buffer the volume change during the charging and discharging processes [12, 13].

This investigation wants to delve into the feasibility of Sn(Li)C, Sn(B)C, Sn(Al)C and Sn(Ga)C nanoclusters for energy storage. Therefore, it was analyzed the physico-chemical properties of mentioned heteroclusters of Sn(Li)C, Sn(B)C, Sn(Al)C and Sn(Ga)C. Following in-depth characterization, samples were measured for their performance correlated with chemical composition varations to legislate their potency for the first time in Li-, B-, Al- or Ga-batteries. These developed anodes are used to make cells with a metal-ion electrolyte using a specific fabrication process.

2 Theory, materials and computation

Alkali metal ion batteries are playing an irreplaceable part in the energy revolution, due to their intrinsic advantages of large capacity/power density and abundance of alkali metal ions in the earth's crust [14].

Despite their great promise, the inborn deficiencies of commercial graphite and other anodes being researched so far call for the quest of better alternatives that exhibit all-round performance with the balance of energy/power density and cycling stability. Fig. 1 shows Sn(Li)C, Sn(B)C, Sn(Al)C and Sn(Ga)C nanoclusters which can enhance the energy storage in battery cells, transistors or other semiconducting devices.

This research has employed the penetration of the hybrid functional of three-parameter basis set of B3LYP (Becke, Lee, Yang, Parr) within the conception of density functional theory (DFT) upon theoretical computations and basis sets of LANL2DZ for metal atoms and 6–311+G(d,p) for other atoms [15, 16].

The analysis of the Bader charge parameter [17] has been illustrated for energy storage by hybrid clusters of Sn(Li)C, Sn(B)C, Sn(Al)C and Sn(Ga)C complexes (Fig. 1) due to multiplicity of +1 and convergence on root mean square (RMS) density matrix = 1.00D-08 and convergence on maximum density matrix = 1.00D-06 by Gaussian 16 revision C.01 computational software [18] and GaussView 6.1 graphical program [19]. The applied basis sets for theoretical calculations of energy storage by Sn(Li)C, Sn(B)C, Sn(Al)C and Sn(Ga)C complexes has been considered LANL2DZ and 6–311+G (d,p) with multiplicity 1.

One of the most significant advantages of applying SnC nanocluster as the anode in Li-, B-, Al- or Ga-batteries is they provide several potential Li/B/Al/Ga-ion storage ways in a stable SnC anode material, increased electrical conductivity from Si/C and surface area from the

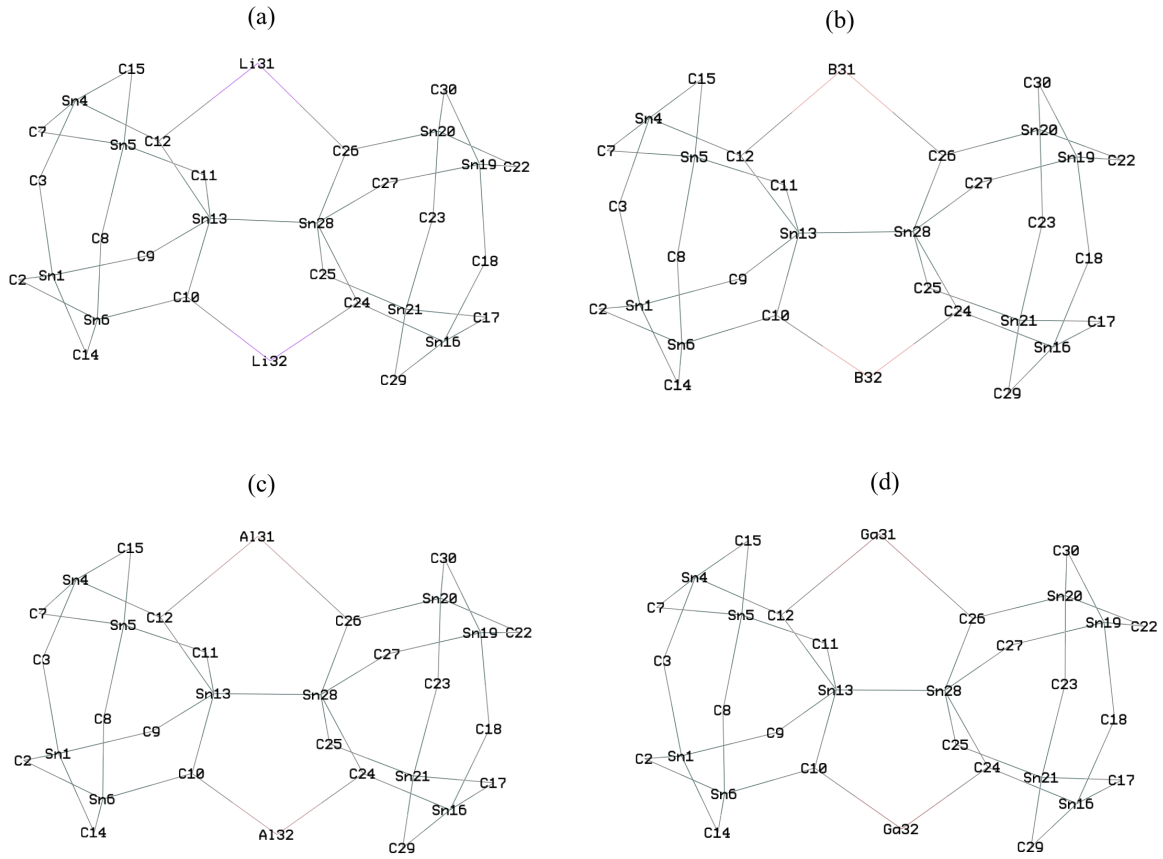

Fig. 1 Replacing Li in (a) Sn(Li)C with B, Al, Ga toward formation of (b) Sn(B)C, (c) Sn(Al)C and (d) Sn(Ga)C complexes, respectively for saving energy as novel batteries

nanocluster morphology. In this investigation, homogenously distributed tin or carbon elements can be immobilized in the SnC matrix, which prevents their tendency to form agglomeration under battery cycling. Scientists have determined that the formation of dendrites on the anode surface not only affects the battery's fading performance but also increases safety risks. The mechanistic models, principles, and influencing factors related to dendrite formation have also supported their precautions. Similarly, theoretically, the morphology of dendrites can be significantly improved by unifying the distribution of electric field and reducing the concentration of metal ions [20].

The Li/B /Al/ Ga insertion might also result in the cleavage of some C–Li, C–B, C–Al or C–Ga bonds in the SnC anode material and the expansion, providing favorable sites for the subsequent ion insertion in the network (Fig. 1). At the same time, the Li, B, Al or Ga atoms could react rapidly with tin or carbide of SnC nanocluster to form Sn(Li)C (Fig. 1(a)), Sn(B)C (Fig. 1(b)), Sn(Al) (Fig. 1(c)) and Sn(Ga)C (Fig. 1(d)) heteroclusters. While focusing on B, Al, Ga-based materials to enhance the electrochemical performance of LBs, we should also explore the theoretical and practical issues involved from the laboratory level to the actual production scale and make a reasonable and comprehensive assessment of the performance of B, Al, Ga-based LBs, so as to provide guidance for the commercialization of LBs.

3 Results and discussion

3.1 Charge density differences analysis

In Fig. 2, charge density differences (CDD) [21] are shown for Sn(Li)C, Sn(B)C, Sn(Al)C and Sn(Ga)C nanoclusters with the vibration in the district about –12 to +9 Bohr through co-interaction between Li31–Li32, and B31–B32, Al31–Al32, Ga31–Ga32. Moreover, the elements of C2, C3, C7–C12, C14, C15, C17, C18, C22–C27, C29, C30 from Sn(Li)C, Sn(B)C, Sn(Al)C and Sn(Ga)C nanoclusters have displayed the vibration about –12 to +9 Bohr (Fig. 2).

The charge distribution is illustrated during atom captured by SnC nanostructure towards formation of Sn(Li)C, Sn(B)C, Sn(Al)C and Sn(Ga)C nanoclusters, respectively (Table 1).

Functionalizing of Li, B, Al, Ga atoms can augment the negative atomic charge of C2, C3, C7–C12, C14, C15, C17, C18, C22–C27, C29, C30 as electron acceptors in Sn(Li)C, Sn(B)C, Sn(Al)C and Sn(Ga)C nanoclusters (Fig. 3).

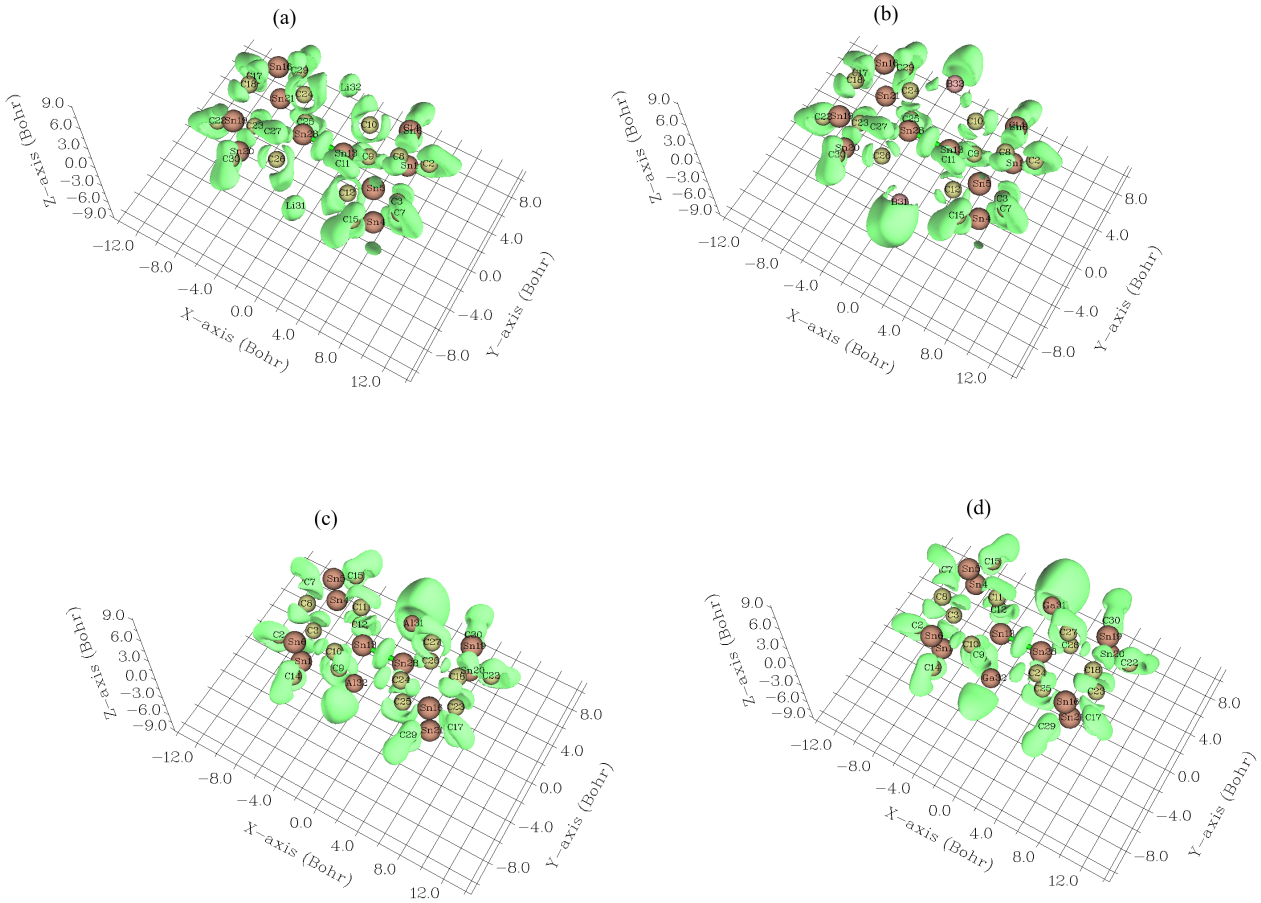

Fig. 2 CDD graphs for (a) Sn(Li)C, (b) Sn(B)C, (c) Sn(Al)C and (d) Sn(Ga)C nanoclusters

The results exhibited that lithium, boron, aluminum and gallium are chemisorbed on the SnC and that electronic charge is transferred from the decorating atom to the the SnC. As can be seen in Fig. 3, the electronic states of carbon sites in SnC near the valence band have an electron acceptor character, while the metal ions sites have an electron donor character.

3.2 Total density of states

In isolated system (such as molecule), the energy levels are discrete, the concept of density of states (DOS) is supposed to be completely valueless in this situation. Therefore, the original total DOS (TDOS) of isolated system can be written as [22]:

$$\mathrm{TDOS}(E)=\sum_i \delta(E-\epsilon_i) \tag{1}$$

The normalized Gaussian function is defined as:

$$G(x)=\frac{1}{c\sqrt{2\pi}}e^{-\frac{x^2}{2c^2}}, \tag{2}$$

where

$$c=\frac{\mathrm{FWHM}}{2\sqrt{2\ln x}}.$$

FWHM (full width at half maximum) is an adjustable parameter in Multiwfn [23, 24]. Furthermore, the curve map of broadened partial DOS (PDOS) and overlap DOS (OPDOS) are valuable for visualizing orbital composition analysis, PDOS function of fragment A is defined as:

$$\mathrm{PDOS}_A(E)=\sum_i \Xi_{i,A}F(E-\epsilon_i) \tag{3}$$

where $\Xi_{i,A}$ is the composition of fragment A in orbital i. The OPDOS between fragment A and B is defined as:

$$\mathrm{OPDOS}_{A,B}(E)=\sum_i \mathrm{X}^i_{A,B}F(E-\epsilon_i) \tag{4}$$

where $\mathrm{X}^i_{A,B}$ is the composition of total cross term between fragment A and B in orbital i.

In the TDOS map, each discrete vertical line corresponds to a molecular orbital (MO), the dashed line highlights the position of highest occupied molecular orbital (HOMO). The curve is the TDOS simulated based on the distribution of MO energy levels.

Table 1 The atomic charge *Q* for Sn(Li)C, Sn(B)C, Sn(Al)C and Sn(Ga)C nanoclusters

Sn(Li)C		Sn(B)C		Sn(Al)C		Sn(Ga)C	
Atom	*Q* (C)	Atom	*Q* (C)	Atom	*Q* (C)	Atom	*Q* (C)
Sn1	0.4767	Sn1	0.4862	Sn1	0.4717	Sn1	0.4775
C2	–0.3183	C2	–0.3111	C2	–0.3101	C2	–0.3125
C3	–0.1790	C3	–0.1907	C3	–0.1789	C3	–0.1750
Sn4	0.4706	Sn4	0.5118	Sn4	0.5036	Sn4	0.5212
Sn5	0.4638	Sn5	0.4800	Sn5	0.4693	Sn5	0.4768
Sn6	0.5113	Sn6	0.5796	Sn6	0.5976	Sn6	0.5955
C7	–0.3102	C7	–0.3151	C7	–0.3084	C7	–0.3107
C8	–0.1559	C8	–0.1766	C8	–0.1601	C8	–0.1573
C9	–0.3352	C9	–0.3053	C9	–0.2842	C9	–0.2898
C10	–0.7357	C10	–0.6164	C10	–1.0599	C10	–0.9601
C11	–0.3444	C11	–0.3306	C11	–0.3075	C11	–0.3158
C12	–0.7635	C12	–0.6278	C12	–0.8745	C12	–0.8173
Sn13	1.4424	Sn13	1.1481	Sn13	1.1911	Sn13	1.2228
C14	–0.3032	C14	–0.2915	C14	–0.2918	C14	–0.2944
C15	–0.3108	C15	–0.2639	C15	–0.2848	C15	–0.2846
Sn16	0.5585	Sn16	0.5794	Sn16	0.5898	Sn16	0.5949
C17	–0.3216	C17	–0.3321	C17	–0.3319	C17	–0.3348
C18	–0.1694	C18	–0.1707	C18	–0.1534	C18	–0.1521
Sn19	0.4356	Sn19	0.4510	Sn19	0.4309	Sn19	0.4369
Sn20	0.4845	Sn20	0.5309	Sn20	0.5355	Sn20	0.5476
Sn21	0.4658	Sn21	0.4772	Sn21	0.4602	Sn21	0.4675
C22	–0.3189	C22	–0.3164	C22	–0.3143	C22	–0.3167
C23	–0.1495	C23	–0.1791	C23	–0.1637	C23	–0.1596
C24	–0.7049	C24	–0.6291	C24	–1.0496	C24	–0.9516
C25	–0.3237	C25	–0.3037	C25	–0.3019	C25	–0.3076
C26	–0.7209	C26	–0.5800	C26	–0.8887	C26	–0.8185
C27	–0.4179	C27	–0.3974	C27	–0.3650	C27	–0.3667
Sn28	1.3792	Sn28	1.1336	Sn28	1.2178	Sn28	1.2303
C29	–0.3228	C29	–0.2753	C29	–0.2973	C29	–0.2952
C30	–0.3155	C30	–0.2775	C30	–0.2989	C30	–0.2981
Li31	0.5219	B31	0.2680	Al31	0.7661	Ga31	0.5978
Li32	0.3115	B32	0.2446	Al32	0.9915	Ga32	0.7499

Regarding energy storage by Sn(Li)C, Sn(B)C, Sn(Al)C and Sn(Ga)C nanoclusters, TDOS has been evaluated. This factor can demonstrate the existence of important chemical interactions often on the convex side (Fig. 4).

Sn(Li)C, Sn(B)C, Sn(Al)C, Sn(Ga)C nanoclusters (Fig. 4) have shown the steepest maximums TDOS surrounding –0.30, –0.40, –0.50 and –0.60 a.u. owing to covalent bond between Li, B, Al, Ga atoms and SnC nanostructure with maximum density of states of ≈12. Substitution engineering is a beneficial method for enhancing the electrochemical performance of electrode materials. In this study, the impact of incorporating various heteroatoms (B, Al, and Ga) instead of Li atoms in SnC nanoclusters on the adsorption of main group metals was thoroughly investigated through first-principles calculations. This analysis aids in evaluating the material's suitability for use in metal ion batteries. Consequently, a single layer of SnC with heteroatom doping exhibits potential as an anode material for metal ion batteries. This research provides insights into how heteroatom decoration influences performance and can be utilized in the development of improved electrodes for rechargeable batteries.

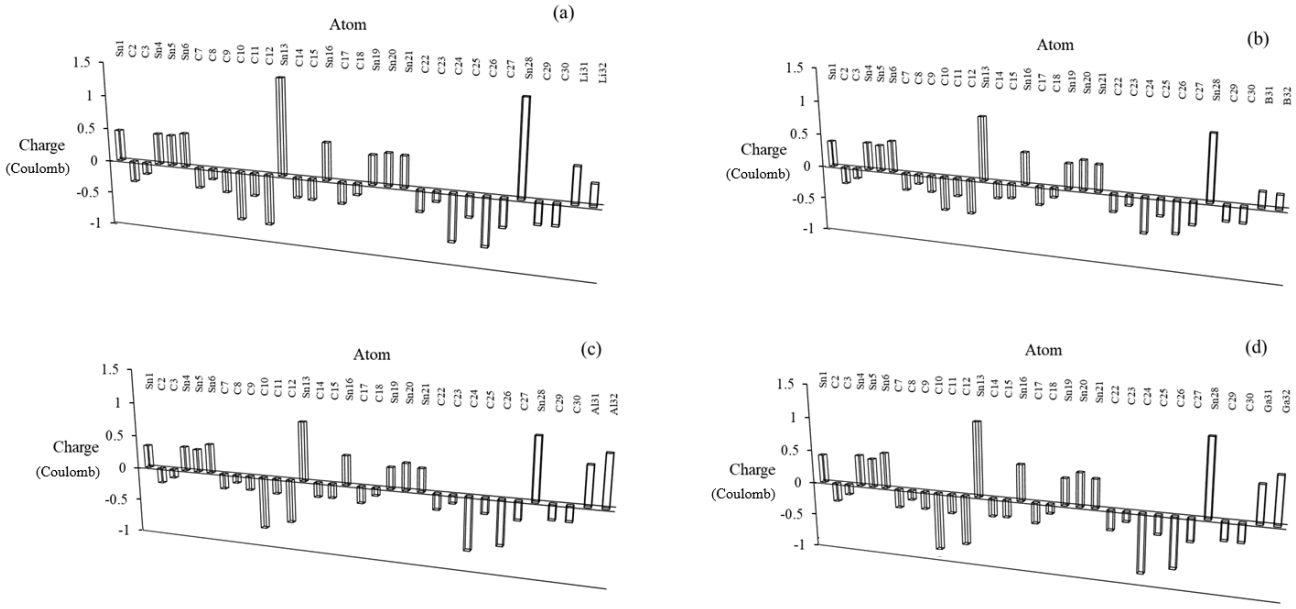

Fig. 3 The changes of charge distribution for (a) Sn(Li)C, (b) Sn(B)C, (c) Sn(Al)C and (d) Sn(Ga)C nanoclusters

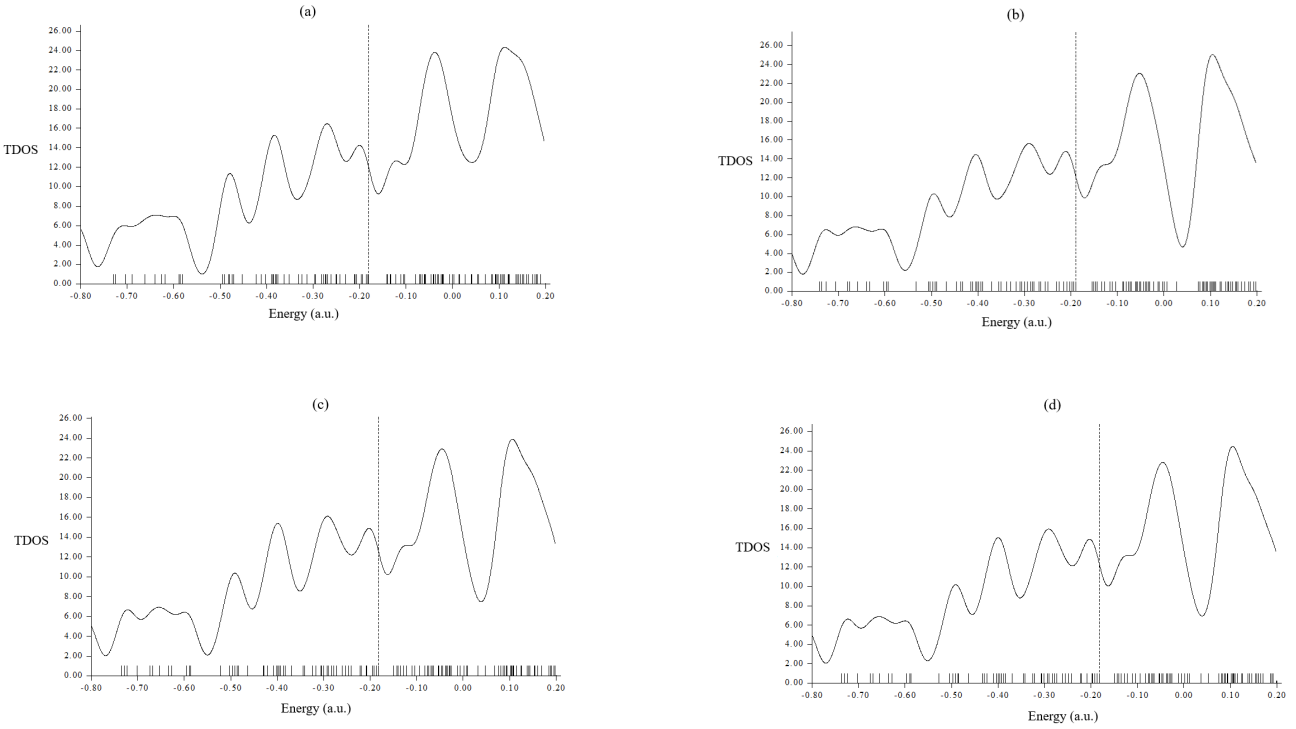

Fig. 4 TDOS graphs of (a) Sn(Li)C, (b) Sn(B)C, (c) Sn(Al)C and (d) Sn(Ga)C nanoclusters

3.3 Electron localization function analysis

A type of scalar fields called electron localization function (ELF) may demonstrate a broad span of bonding samples. Nevertheless, the distinction between deduced/raised electron delocalization/localization into cyclic π-conjugated sets stays encouraging for ELF [25]. The grosser the electron localization is in an area, the more likely the electron movement is restricted within it. Therefore, they might be discerned from the ones away if electrons are totally centralized. As Bader investigated, the zones with large electron localization possess extensive magnitudes of Fermi hole integration [26]. But, with having a six-dimension function for the Fermi hole, it seems hard to be studied directly. Then, Becke and Edgecombe remarked

that spherically averaged like spin conditional pair probability possesses a direct correlation with the Fermi hole and proposed the parameter of ELF in Multiwfn program [23, 24] and popularized for spin-polarized procedure [27]. Regarding kinetic energy, ELF was rechecked to be more punctual for both Kohn-Sham DFT and post-Hartree-Fock (post-HF) wavefunctions [28].

Trapping of Li, B, Al, Ga atoms by SnC nanostructure (Fig. 5) towards formation of Sn(Li)C, Sn(B)C, Sn(Al)C and Sn(Ga)C nanoclusters might be described by ELF graphs using Multiwfn [23, 24] due to achieving their delocalization/localization characterizations [25] of electrons and chemical bonds (Fig. 5).

Sn(Li)C (Fig. 5(a)), Sn(B)C (Fig. 5(b)), Sn(Al)C (Fig. 5(c)), Sn(Ga)C (Fig. 5(d)) have demonstarted the electron delocalization through an isosurface map with labeling atoms of C10, C12, Si13, C24, C26, Si28, X31/X32 (X = Li, B, Al, Ga). In fact, the counter map of ELF can confirm that Sn(Li)C, Sn(B)C, Sn(Al)C and Sn(Ga)C nanoclusters may augment the efficiency of energy storage (Fig. 5).

Besides, intermolecular orbital overlap integral is important in illustration of intermolecular charge transfer which can compute HOMO-HOMO and LUMO-LUMO (lowest unoccupied molecular orbital) overlap integrals between Li, B, Al, Ga atoms and SnC nanostructure. The layered tin carbide improved by lithium, boron, aluminum and gallium have indicated the structural stability of Li-, B-, Al-, and Ga ion batteries through the reported stability energies in Table 2.

Battery capacity indicates the amount of charge or energy a battery can store, reflecting the electricity generated from the chemical reactions within the battery. It is also referred to as battery charge capacity and is measured in ampere-hours (Ah). Nominal capacity denotes the performance of a new battery under specific, controlled

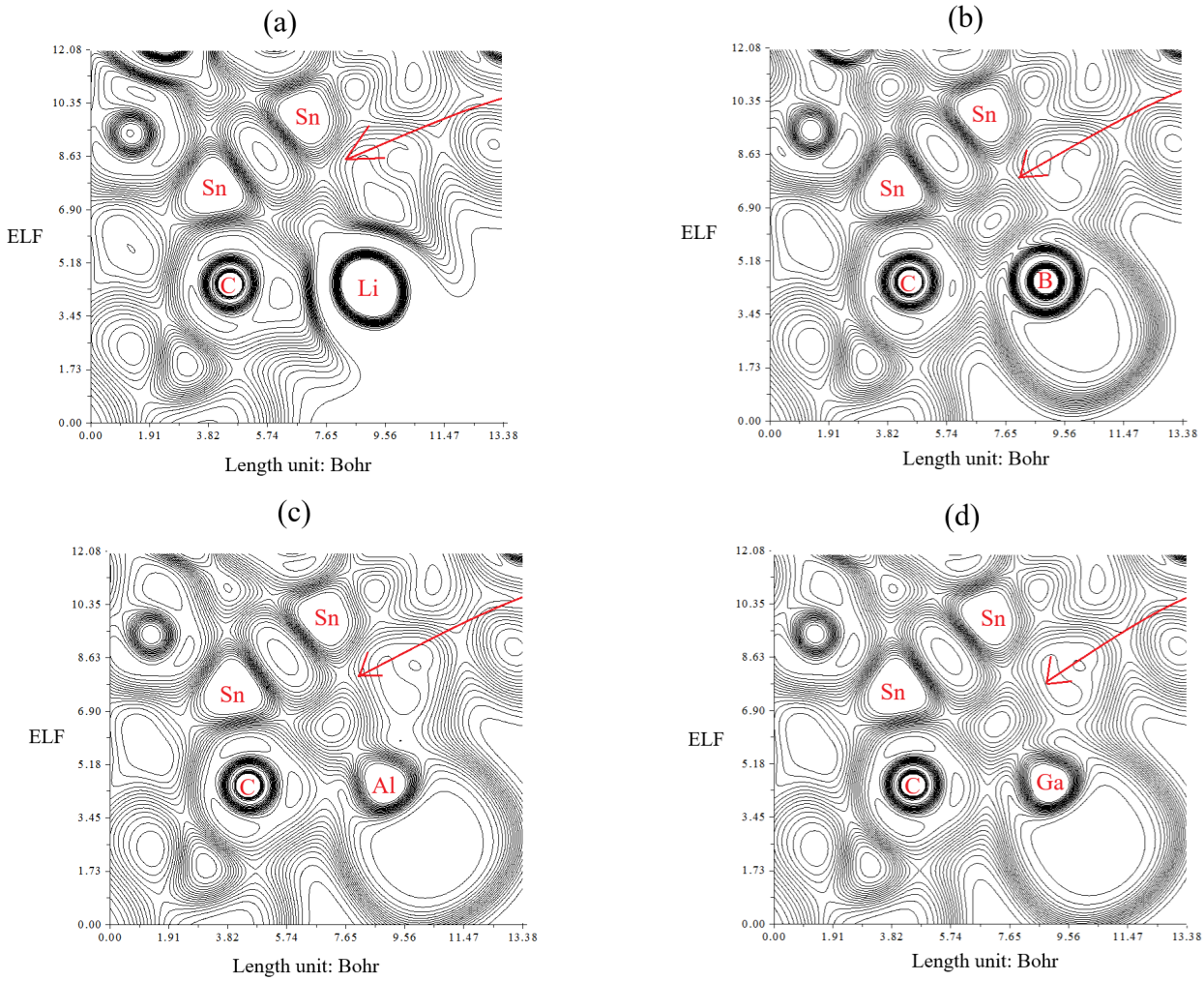

Fig. 5 The counter maps of ELF graphs for (a) Sn(Li)C, (b) Sn(B)C, (c) Sn(Al)C and (d) Sn(Ga)C nanoclusters

Table 2 Stability energy E_s, dipole moment, HOMO and LUMO energy levels, E_{HOMO} and E_{LUMO} energy gap (ΔE) and cell capacity Cfor Sn(Li)C, Sn(B)C, Sn(Al)C and Sn(Ga)C nanoclusters

Heteroclusters	$E_s \times 10^{-3}$ (kcal/mol)	Dipole moment (debye)	E_{HOMO} (eV)	E_{LUMO} (eV)	$\Delta E = E_{LUMO} - E_{HOMO}$ (eV)	C (mAh g^{-1})
Sn(Li)C	−503.7086	1.2033	−4.9308	−3.8369	1.0938	370.6956
Sn(B)C	−525.2624	0.9578	−5.1668	−4.1947	0.9720	1055.5851
Sn(Al)C	−496.7349	1.4554	−4.9550	−4.0654	0.8896	870.7198
Sn(Ga)C	−496.8159	1.3504	−4.9707	−4.0702	0.9005	595.2203

conditions. Battery state-of-charge indicates the current charge level compared to when the battery is fully charged. Lastly, battery state-of-health provides insight into the overall condition and performance of the battery as time progresses [29, 30]:

$$C = \frac{nF}{3600 \times M} \tag{5}$$

where F, n and M are Faraday constants, the metal charge numbers for Li(+1), and B, Al, Ga(+3) and the molecular mass, respectively, in the mentioned nanoclusters.

Moreover, intermolecular orbital overlap integral is important in discussions of intermolecular charge transfer which can calculate HOMO-HOMO and LUMO-LUMO overlap integrals between the metal/metalloids and tin carbide. The wavefunction level we used to be CAM–B3LYP–D3/6–311+G(d,p) that correspond to HOMO and LUMO, respectively (Table 2). Therefore, E_{LUMO} (a.u.), E_{LUMO} (a.u.) and the local bandgap energies ΔE (a.u.) and immobile charges induced by polarization discontinuity are simultaneously controlled throughout the structures, and optimized band profiles are eventually achieved for Sn(Li)C, Sn(B)C, Sn(Al)C and Sn(Ga)C nanoclusters (Table 2). Energy gap $\Delta E = (E_{LUMO} - E_{HOMO})$ has shown the positive chemical potential mainly related to stability. When the softness is lower than hardness, this means the compounds are highly stable. The smaller the energy gap ΔE the greater the reactivity of a molecule. Therefore, replacing Li in Sn(Li)C with boron group consisting of B, Al or Ga can enhance the potential utility of Sn(B)C, Sn(Al)C and Sn(Ga)C nanoclusters in battery energy storage (Table 2).

In addition, the amount of theMayer bond order [31] is generally according to empirical bond order for the single bond is near 1.0. The Mulliken bond order [32] with a small accord with empirical bond order is not appropriate for quantifying bonding strength, for which the Mayer bond order always performs better. However, the Mulliken bond order is a good qualitative indicator for positive amount of bonding and negative amount of antibonding which are evacuated and localized, respectively (Table 3).

As it is seen in Table 3, the Laplacian bond order [33] has a straight cohesion with bond polarity, bond dissociation energy and bond vibrational frequency. The low value of Laplacian bond order might demonstrate that it is insensitive to the calculation degree applied for producing electron density. Generally, the value of the Fuzzy bond order is near the Mayer bond order, especially for low-polar bonds, but much more stable with respect to the change in basis-set. Computation of the Fuzzy bond order demands running the Becke's DFT numerical integration, owing to which the calculation value is larger than assessment of the Mayer bond order and it can concede more precisely [34]. In the Fuzzy nanoclustering sample, these intervals are additionally weighted by membership degrees. The more accurately data objects are assigned to nanoclusters, the smaller the error and the higher the density. However, this measurement does not explicitly consider the separation of different clusters.

4 Conclusions

Boron group atoms captured by tin carbide towards the formation of Sn(B)C, Sn(Al)C and Sn(Ga)C nanoclusters were studied by computational methods through a qualitative screening. The changes in charge density are defined as a notable charge transfer in Sn(B)C, Sn(Al)C and Sn(Ga)C. Due to the semiconducting nature of SnC, it is usually composited with C for better ionic and electronic conductivities. It is well established that enhancing B, Al or Ga to cell batteries can augment the energy saving properties of cell batteries. This research article is useful for designing and constructing Li, B, Al, or Ga hybrid batteries with high power density/energy density with excellent cycle stability and will represent a perspective for the industrial application of these hybrid batteries. The improvement of the interfacial properties of LBs is essential in solving the corresponding problems encountered in their further development, so it needs to be studied in depth how to design and optimize the structure of B, Al, Ga-containing electrolyte additives, Li salts, and binder to meet the requirements of long cycle and high voltage conditions.

Table 3 The bond order of Mayer, Wiberg, Mulliken, Laplacian and Fuzzy from mixed alpha and beta density matrix for Sn(B)C, Sn(Al)C, and Sn(Ga)C nanoclusters

Compound	Bond type	Bond order				
		Mayer	Wiberg	Mulliken	Laplacian	Fuzzy
Sn(Li)C	Sn13–Sn28	0.1891	0.5161	0.5038	0.3628	0.8467
	C10–Li32	0.5217	0.4497	0.6241	0.2618	0.3128
	C12–Li31	0.2895	0.2908	0.3063	0.3457	0.1558
	C24–Li32	0.4818	0.4303	0.5560	0.5996	0.2974
	C26–Li31	0.3234	0.3450	0.3555	0.3916	0.1998
Sn(B)C	Sn13–Sn28	0.3404	0.5575	0.6978	0.4734	0.8720
	C10–B32	0.9459	0.9910	0.5483	0.1623	0.7232
	C12–B31	0.4263	0.5546	0.1982	0.3697	0.3748
	C24–B32	0.9476	0.9698	0.5946	0.1377	0.7031
	C26–B31	0.5296	0.6947	0.1126	0.2324	0.4808
Sn(Al)C	Sn13–Sn28	0.4618	0.5760	0.3156	0.5063	0.8637
	C10–Al32	0.7791	0.8777	0.5080	0.3217	0.8259
	C12–Al31	0.3964	0.5072	0.1206	0.3220	0.4534
	C24–Al32	0.7786	0.8526	0.5789	0.2719	0.8009
	C26–Al31	0.4567	0.6285	0.1499	0.1798	0.5636
Sn(Ga)C	Sn13–Sn28	0.3959	0.5758	0.4141	0.5020	0.8447
	C10–Ga32	0.9117	0.8986	0.6112	0.4302	0.8739
	C12–Ga31	0.4313	0.5119	0.1634	0.3429	0.4810
	C24–Ga32	0.9102	0.8746	0.6780	0.3608	0.8513
	C26–Ga31	0.5068	0.6363	0.2131	0.1714	0.5909

Acknowledgements

The authors are grateful to Kastamonu University for completing this paper and its research.

References

[1] Liang, S., Cheng, Y.-J., Zhu, J., Xia, Y., Müller-Buschbaum, P. "A Chronicle Review of Nonsilicon (Sn, Sb, Ge)-Based Lithium/Sodium-Ion Battery Alloying Anodes", Small Methods, 4(8), 2000218, 2020. https://doi.org/10.1002/smtd.202000218

[2] Ma, L., Tan, J., Wang, Y., Liu, Z., Yang, Y., Gray, T., Zhang, X., Ye, M., Shen, J. "Boron-Based High-Performance Lithium Batteries: Recent Progress, Challenges, and Perspectives", Advanced Energy Materials, 13(25), 2300042, 2023. https://doi.org/10.1002/aenm.202300042

[3] Shahzad, K., Cheema, I. I. "Aluminum batteries: Unique potentials and addressing key challenges in energy storage", Journal of Energy Storage, 90, 111795, 2024. https://doi.org/10.1016/j.est.2024.111795

[4] Zhang, B.-W., Ren, L., Wang, Y.-X., Xu, X., Du, Y., Dou, S.-X. "Gallium-based liquid metals for lithium-ion batteries", Interdisciplinary Materials, 1(3), pp. 354–372, 2022. https://doi.org/10.1002/idm2.12042

[5] Mollaamin, F., Monajjemi, M. "Electric and Magnetic Evaluation of Aluminum–Magnesium Nanoalloy Decorated with Germanium Through Heterocyclic Carbenes Adsorption: A Density Functional Theory Study", Russian Journal of Physical Chemistry B, 17(3), pp. 658–672, 2023. https://doi.org/10.1134/S1990793123030223

[6] Mollaamin, F. "Competitive Intracellular Hydrogen-Nanocarrier Among Aluminum, Carbon, or Silicon Implantation: a Novel Technology of Eco-Friendly Energy Storage using Research Density Functional Theory", Russian Journal of Physical Chemistry B, 18(3), pp. 805–820, 2024. https://doi.org/10.1134/S1990793124700131

[7] Mollaamin, F. "Alkali Metals Doped on Tin-Silicon and Germanium-Silicon Oxides for Energy Storage in Hybrid Biofuel Cells: A First-Principles Study", Russian Journal of Physical Chemistry B, 19(3), pp. 722–736, 2025. https://doi.org/10.1134/S1990793125700393

[8] Montoya-García, A. R., Cid, B. J., Arellano, L. G., Miranda, Á., Fernando Salazar, F., Pérez, L. A., Cruz-Irisson, M. "The effect of doping on hydrogen storage in alkali-adatoms SnC nanosheet: A DFT study", International Journal of Hydrogen Energy, 161, 150709, 2025. https://doi.org/10.1016/j.ijhydene.2025.150709

[9] Shahzad, R. F., Rasul, S., Mamlouk, M., Lukose, C. C., Shakoor, R. A., Zia, A. W. "Innovative Tin and hard carbon architecture for enhanced stability in lithium-ion battery anodes", Journal of Energy Storage, 100, 113671, 2024. https://doi.org/10.1016/j.est.2024.113671

[10] Tomboc, G. M., Wang, Y., Wang, H., Li, J., Lee, K. "Sn-based metal oxides and sulfides anode materials for Na ion battery", Energy Storage Materials, 39, pp. 21–44, 2021. https://doi.org/10.1016/j.ensm.2021.04.009

[11] Marcos-Viquez, A. L., Miranda, A., Cruz-Irisson, M., Pérez, L. A. "Tin carbide monolayers decorated with alkali metal atoms for hydrogen storage", International Journal of Hydrogen Energy, 47(97), pp. 41329–41335, 2022. https://doi.org/10.1016/j.ijhydene.2021.12.204

[12] An, Y., Tian, Y., Wei, C., Jiang, H., Xi, B., Xiong, S., Feng, J., Qian, Y. "Scalable and Physical Synthesis of 2D Silicon from Bulk Layered Alloy for Lithium-Ion Batteries and Lithium Metal Batteries", ACS Nano, 13(12), pp. 13690–13701, 2019. https://doi.org/10.1021/acsnano.9b06653

[13] Mollaamin, F., Monajjemi, M. "Nanomaterials for Sustainable Energy in Hydrogen-Fuel Cell: Functionalization and Characterization of Carbon Nano-Semiconductors with Silicon, Germanium, Tin or Lead through Density Functional Theory Study", Russian Journal of Physical Chemistry B, 18(2), pp. 607–623, 2024. https://doi.org/10.1134/S1990793124020271

[14] Mollaamin, F. "Anchoring of 2D layered materials of $Ge_5Si_5O_{20}$ for (Li/Na/K)-(Rb/Cs) batteries towards Eco-friendly energy storage", BMC Chemistry, 19(1), 233, 2025. https://doi.org/10.1186/s13065-025-01593-0

[15] Becke, A. D. "Density-functional thermochemistry. III. The role of exact exchange", The Journal Chemical Physics, 98(7), pp. 5648–5652, 1993. https://doi.org/10.1063/1.464913

[16] Lee, C., Yang, W., Parr, R. G. "Development of the Colle–Salvetti correlation-energy formula into a functional of the electron density", Physical Review B, 37(2), pp. 785–789, 1988. https://doi.org/10.1103/PhysRevB.37.785

[17] Henkelman, G., Arnaldsson, A., Jónsson, H. "A fast and robust algorithm for Bader decomposition of charge density", Computational Materials Science, 36(3), pp. 354–360, 2006. https://doi.org/10.1016/j.commatsci.2005.04.010

[18] M. J. Frisch, G. W. Trucks, H. B. Schlegel, G. E. Scuseria, M. A. Robb, ..., D. J. Fox, Gaussian 16, Revision C.01, Gaussian, Inc., Wallingford CT, 2016.

[19] R. Dennington, T. A. Keith, J. M. Millam, "GaussView (Version 6.06.16)", [computer program] Semichem Inc., Shawnee Mission, KS, 2016. Available at: url [Accessed: Day Month Year]

[20] Aslam, M. K., Niu, Y., Hussain, T., Tabassum, H., Tang, W., Xu, M., Ahuja, R. "How to avoid dendrite formation in metal batteries: Innovative strategies for dendrite suppression", Nano Energy, 86, 106142, 2021. https://doi.org/10.1016/j.nanoen.2021.106142

[21] Xu, Z., Qin, C., Yu, Y., Jiang, G.., Zhao, L. "First-principles study of adsorption, dissociation, and diffusion of hydrogen on α-U (110) surface", AIP Advances, 14(5), 055114, 2024. https://doi.org/10.1063/5.0208082

[22] Rukelj, Z., Kupčić, I., Radić, D. "Density of States in the 3D System with Semimetallic Nodal-Loop and Insulating Gapped Phase", Symmetry, 16(1), 38, 2024. https://doi.org/10.3390/sym16010038

[23] Lu, T., Chen, F. "Multiwfn: A multifunctional wavefunction analyzer", Journal of Computational Chemistry, 33(5), pp. 580–592, 2012. https://doi.org/10.1002/jcc.22885

[24] Lu, T. "A comprehensive electron wavefunction analysis toolbox for chemists, Multiwfn", The Journal of Chemical Physics, 161(8), 082503, 2024. https://doi.org/10.1063/5.0216272

[25] Matta, C. F., Ayers, P. W., Cook, R. "The Physics of Electron Localization and Delocalization", In: Electron Localization-Delocalization Matrices, Springer Cham, 2024, pp. 7–20. ISBN 978-3-031-51434-0 https://doi.org/10.1007/978-3-031-51434-0_2

[26] Bader, R. F. W. "The zero-flux surface and the topological and quantum definitions of an atom in a molecule", Theoretical Chemistry Accounts, 105(4), pp. 276–283, 2001. https://doi.org/10.1007/s002140000233

[27] Becke, A. D., Edgecombe, K. E. "A simple measure of electron localization in atomic and molecular systems", The Journal of Chemical Physics, 92(9), pp. 5397–5403, 1990. https://doi.org/10.1063/1.458517

[28] Savin, A., Jepsen, O., Flad, J., Flad, J., Andersen, O. K., Preuss, H., von Schnering, H. G. "Electron Localization in Solid-State Structures of the Elements: the Diamond Structure", Angewandte Chemie International Edition, 31(2), pp. 187–188, 1992. https://doi.org/10.1002/anie.199201871

[29] Wu, S., Ren, M. "Industrial Basic Capacity Research: Theory and Measurement", Systems, 12(11), 502, 2024. https://doi.org/10.3390/systems12110502

[30] Bašić, H., Bobanac, V., Pandžić, H. "Determination of Lithium-Ion Battery Capacity for Practical Applications", Batteries, 9(9), 459, 2023. https://doi.org/10.3390/batteries9090459

[31] Mayer, I. "Improved definition of bond orders for correlated wave functions", Chemical Physics Letters, 544, pp. 83–86, 2012. https://doi.org/10.1016/j.cplett.2012.07.003

[32] Ertural, C., Steinberg, S., Dronskowski, R. "Development of a robust tool to extract Mulliken and Löwdin charges from plane waves and its application to solid-state materials", RSC Advances, 9(51), pp. 29821–29830, 2019. https://doi.org/10.1039/c9ra05190b

[33] Lu, T., Chen, F. "Bond Order Analysis Based on the Laplacian of Electron Density in Fuzzy Overlap Space", The Journal of Physical Chemistry A, 117(14), pp. 3100–3108, 2013. https://doi.org/10.1021/jp4010345

[34] Wang, X., Zhang, X., Pedrycz, W., Yang, S.-H., Boutat, D. "Consensus of T-S Fuzzy Fractional-Order, Singular Perturbation, Multi-Agent Systems", Fractal and Fractional, 8(9), 523, 2024. https://doi.org/10.3390/fractalfract8090523